ACS Macro Letters

pubs.acs.org/macroletters Letter

# A Thermodynamic Roadmap for the Grafting-through Polymerization of $PDMS_{11}MA$

Michael R. Martinez, Yidan Cong, Sergei S. Sheiko, and Krzysztof Matyjaszewski*

Cite This: *ACS Macro Lett.* 2020, 9, 1303−1309 Read Online

ACCESS | Metrics & More | Article Recommendations | Supporting Information

**ABSTRACT:** Grafting-through atom transfer radical polymerization (ATRP) was used to polymerize a sterically hindered poly(dimethylsiloxane) methacrylate ($PDMS_{11}MA$, $M_n$ = 1000) macromonomer to high conversion as a function of temperature, solvent, initial monomer concentration, and pressure. Higher polymerization yields were obtained when polymerizations were conducted at (i) lower temperature ($T$), (ii) in a poor solvent for the side chain, (iii) higher initial monomer concentration ($[M]_0$), and (iv) higher pressure by mitigating the contribution of the equilibrium monomer concentration ($[M]_{eq}$). The enthalpy of polymerization ($\Delta H_p$) and entropy of polymerization ($\Delta S_p$) were more negative in poor solvents. Polymerizations at ambient pressure required higher $[M]_0$, use of a poor solvent, and lower temperatures to reach higher conversion with good control, whereas high pressure ATRP (HP-ATRP) displayed better control under dilute conditions. Grafting-through polymerization at high $P$ and higher $[M]_0$ was less controlled, plausibly due to limited solubility and mobility of the copper catalyst in the highly viscous medium.

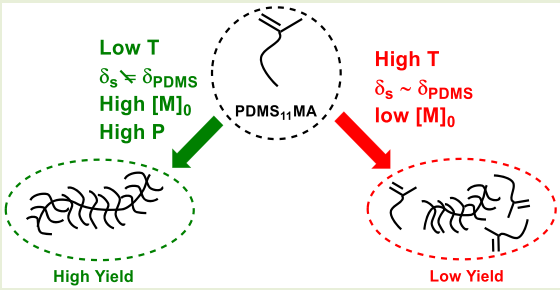




Bottlebrush polymers represent a distinct class of polymer architectures that consist of a long polymer backbone with densely grafted side chains.[1−3] Brush architecture can be tuned through the degree of polymerization (DP) of side chains, main chain, and grafting density. These factors influence the molecular conformation and physical properties of bottlebrush polymers in melt, cross-linked, and gel states.[4−9] Molecular bottlebrushes could be prepared by the "grafting-onto" (grafting side chains onto a functionalized backbone),[10,11] "grafting-through" (polymerizing macromonomers),[12−16] or "grafting-from" (growing side chains from a macroinitiator backbone) methods.[17−19]

Grafting-through radical polymerization of methacrylic macromonomers is synthetically challenging because steric repulsion between bulky side chains results in a less negative enthalpy of polymerization ($\Delta H_p$) due to bond stretching and bond-angle deformation.[20] Additionally, side chain bulk generally decreases the entropy of polymerization ($\Delta S_p$). This yields a smaller gain in free energy of polymerization ($\Delta G_p$) under most polymerization conditions and generates competition between grafting-through polymerization and its reverse reaction, depolymerization.[12,21] The equilibrium monomer concentration ($[M]_{eq}$) is the concentration of monomer at a thermodynamic equilibrium where the rate of propagation is equal to the rate of depropagation ($R_p = R_{dp}$).[20,22−25] The concentration of reactant (monomer) and product (bottlebrush) at equilibrium is affected by reaction temperature ($T$), according to eq 1. The nonstandard state $\Delta S_p$ is related to the standard state $\Delta S_p^0$ by $\Delta S_p = \Delta S_p^0 + R \ln \frac{[M]_0}{c}$, where $c$ is the standard-state concentration (1 M).[21,26]

$$\ln([M]_{eq}) = \frac{\Delta H_p}{RT} - \frac{S_p^0}{R} \quad (1)$$

Reversibility of a grafting-through polymerization can be observed in three different ways, depending on the reaction conditions and initial monomer concentration ($[M]_0$).

(i) In a solution of monomer and solvent at $[M]_0 < [M]_{eq}$, no polymerization occurs.[12]
(ii) In a solution of monomer and solvent at $[M]_0 > [M]_{eq}$, polymerization occurs until conversion reaches a plateau at $[M] = [M]_{eq}$.[12,21,25,27]
(iii) In a solution of polymer, polymer chains may depolymerize after appropriate activation until $[M] = [M]_{eq}$.[21,25]

Both propagation and depropagation reactions should be kinetically favorable for thermodynamic effects to be noticeable. Inhibitors, oxygen, or a loss of initiators or catalysts to create radicals, will inhibit both polymerization and depolymerization.[21] Similarly, excessive termination can stop

Received: May 6, 2020
Accepted: August 20, 2020

   https://dx.doi.org/10.1021/acsmacrolett.0c00350
*ACS Macro Lett.* 2020, 9, 1303−1309

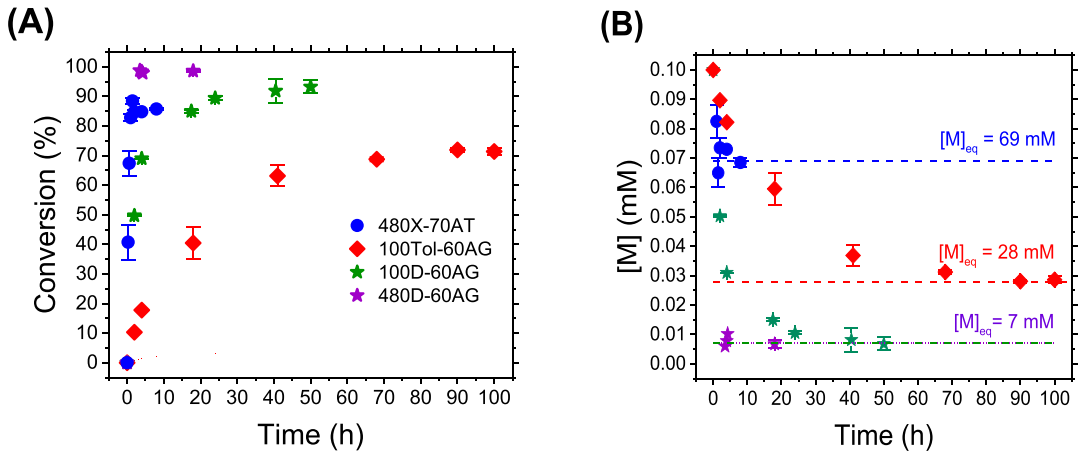


**Figure 1.** (A) Monomer conversion as a function of time for 480X-70AT, 100Tol-60AG, 100D-60AG, and 480D-60AG. (B) Monomer concentration as a function of time for 480X-70AT, 100Tol-60AG, 100D-60AG, and 480D-60AG. Normal ATRP conditions: [$PDMS_{11}MA$]/[df-EBiB]/[CuCl]/[$Me_6$TREN] = [500]/[1]/[4]/[4] in xylene at $[M]_0$ = 480 mM and $T$ = 70 °C. AGET ATRP conditions: [$PDMS_{11}MA$]/[EBiB]/[$CuBr_2$]/[PMDETA]/[$Sn(EH)_2$] = [50]/[1]/[1]/[3]/[1] at $T$ = 60 °C in the stated solvent and scaled to the stated $[M]_0$.

a polymerization or depolymerization reaction before [M] reaches $[M]_{eq}$ at a dead-end monomer concentration $[M]_\infty$, since radicals can no longer be generated to push equilibrium in one direction or the other.

$[M]_{eq}$ in a grafting-through ATRP places an upper limit of polymer yield and can slow the rate of polymerization relative to transfer and termination reactions as [M] approaches $[M]_{eq}$.[27] This can increase dispersity and diminish chain end functionality. Additionally, the presence of residual macromonomer in polymer brushes can cause ill-defined plasticization and leaching effects, because removal of large macromonomers from a mixture with chemically identical polymer brushes is difficult. Thus, $[M]_{eq}$ should be minimized in grafting-through polymerizations to increase reaction yield, reaction rate, and product purity.

The effects of $[M]_{eq}$ are minimized when polymerizations are conducted at lower $T$ and higher $[M]_0$ since a larger fraction of monomer can be polymerized before [M] = $[M]_{eq}$.[27] Polymerization at high pressure also lowers the $[M]_{eq}$.[28] Other parameters, such as solvent and initial concentration of reagents, can also affect $[M]_{eq}$.[29,30] The thermodynamics of polymerization are related to an equilibrium of mixing in solution and depend on the respective monomer−solvent, polymer−solvent, and monomer−polymer interactions.[30−34] The $[M]_{eq}$ of the cationic polymerization of tetrahydrofuran (THF) at 25 °C has a linear dependence with solvent fraction and $[M]_0$, where $[M]_{eq}$ is highest at low $[M]_0$ in more acidic solvents, which strongly interact with monomer THF.[34−36] Macromonomers are chemically very similar to poly(macromonomer)s ($X_{mp}$ ∼ 0.5), but exhibited a strong solvent-dependence in polymerizability, plausibly due to differences in swelling and conformations between the macromonomer and bottlebrush.[37] Grafting-through radical polymerizations of poly(ethylene glycol) methyl ether methacrylate (OEOMA) macromonomers were more exothermic and exoentropic when conducted in poor solvents with a larger difference in the Hansen solvent parameter of the solvent and macromonomer/brush side chain $(\delta_P - \delta_s)^2$. This led to a higher yield in grafting-through polymerizations at lower temperatures. $[M]_{eq}$ in a grafting-through polymerization can also be suppressed by copolymerization with comonomer "diluents" to alleviate steric hindrance between side chains at the cost of grafting density and a potential shift from ideal rheology if stiffness of the spacer is different than the side chains.[4,15,38,39]

This manuscript aims to explore and exploit solvent selection, $[M]_0$, and pressure to reach higher conversion in polymerizations of monomethacryloxypropyl-terminated poly(dimethylsiloxane) ($PDMS_{11}MA$) of $M_n$ = 1000 by suppression of $[M]_{eq}$. This macromonomer contains a *n*-butyl tail, followed by an average of 10 $SiMe_2O$ repeat units, an additional $SiMe_2$ unit needed for hydrosilylation, and then a *n*-propyl carbon spacer before the methacrylate headgroup. Thus, the length of the side group consists of 28 atoms and can be defined as the analogue to 14 monomeric vinyl units (Figure S1). The thermodynamic limit of P(PDMSMA) was recently exploited to partially depolymerize short P($PDMS_7MA$) and P($PDMS_{70}MA$) bottlebrushes.[21] Polymer networks and thermoplastic elastomers based on P(PDMSMA) have received widespread attention as supersoft elastomers that mimic biological softness and strain-hardening.[40,41] Despite this interest, there is a lack of mechanistic investigation into the thermodynamic barriers of grafting-through RP to reach high conversion.

Polymerization experiments are titled in the format MS-T-P, where S refers to the solvent (X = xylene, Tol = toluene, C = chlorobenzene, and D = dioxane), M is $[M]_0$ in units of mM, T is the reaction temperature (°C), and P is the pressure in kbar. Polymerizations by activator generation by electron transfer ATRP (AGET ATRP), which utilizes electron transfer with a tin(II) ethyl hexanoate ($Sn(EH)_2$) reducing agent to regenerate $Cu^{(I)}Br$, are denoted with the postscript "AG".[42] Normal ATRP is denoted by the postscript "AT". Pressure is not denoted for reactions conducted at ambient pressure. Solvents were selected on the basis of their solubility parameters, where a more chemically different solvent to PDMS was expected to increase the polymerization yield. Xylene is the most chemically similar solvent to the PDMS ($(\delta_P - \delta_s)^2$ = 1.69), followed by toluene ($(\delta_P - \delta_s)^2$ = 2.56), chlorobenzene ($(\delta_P - \delta_s)^2$ = 9), and dioxane ($(\delta_P - \delta_s)^2$ = 9.61) (Table S7). Polymerizations at high pressure were conducted in xylene at varying $[M]_0$ from 1 bar to 4.2 kbar to elucidate kinetic and thermodynamic trends in grafting-through polymerization at ambient and high pressure.


https://dx.doi.org/10.1021/acsmacrolett.0c00350
ACS Macro Lett. 2020, 9, 1303−1309

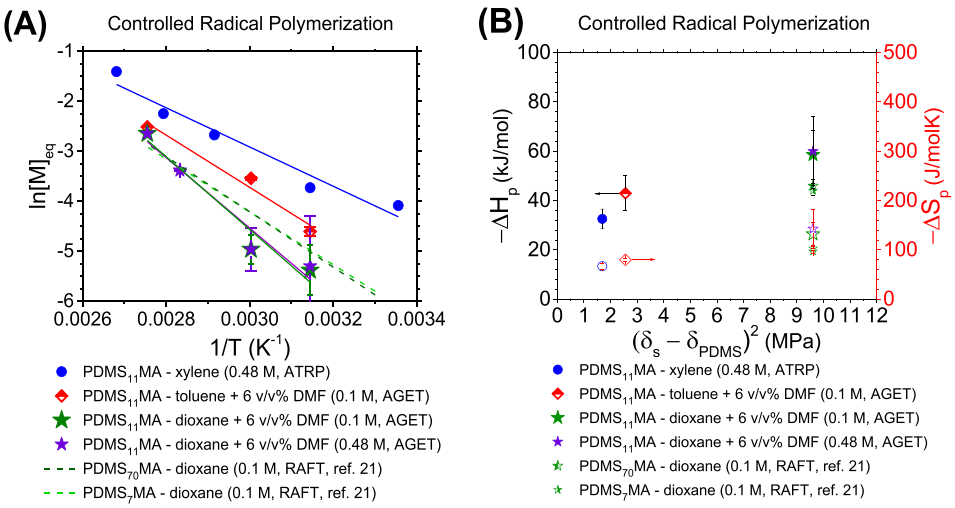


**Figure 2.** (A) Plot of $\ln[M]_{eq}$ vs $1/T$ for controlled radical polymerizations of PDMSMA macromonomers. (B) $-\Delta H_p$ and $-\Delta S_p$ against $(\delta_s - \delta_{PDMS})^2$ for controlled radical polymerizations. Closed symbols correspond to $-\Delta H_p$ and open symbols are $-\Delta S_p$. Normal ATRP conditions: $[PDMS_{11}MA]/[df\text{-}EBiB]/[CuCl]/[Me_6TREN] = [500]/[1]/[4]/[4]$ in xylene at $[M]_0 = 480$ mM. AGET ATRP conditions: $[PDMS_{11}MA]/[EBiB]/[CuBr_2]/[PMDETA]/[Sn(EH)_2] = [50]/[1]/[1]/[3]/[1]$ in the stated solvent and scaled to the stated $[M]_0$. RAFT data of $PDMS_7MA$ and $PDMS_{70}MA$ at $[M]_0 = 100$ mM from ref 21. Solubility parameters were collected from literature and are given in Table S7.

**Table 1. Thermodynamic Parameters of Radical Polymerization for PDMSMA Macromonomers**

| monomer | solvent | $[M]_0$ (mM) | method | $[M]_{\infty,60°C}$ (mM) | $(\delta_P - \delta_s)^2$ [a] | $-\Delta H_p$ (kJ/mol) | $-\Delta S_p$ [b] (J/mol·K) | $R^2$ |
|---|---|---|---|---|---|---|---|---|
| $PDMS_{11}MA$ | xylene | 480 | ATRP | 43 [c,d] | 1.69 | 32.6 ± 4 | 67 ± 6 | 0.94 |
| $PDMS_{11}MA$ | toluene + 6 vol % DMF | 100 | AGET ATRP | 28 ± 1 [c] | 2.56 | 43 ± 7 | 80 ± 3 | 0.94 |
| $PDMS_{11}MA$ | dioxane + 6 vol % DMF | 100 | AGET ATRP | 7 ± 3 [c] | 9.61 | 60 ± 14 | 143 ± 40 | 0.90 |
| $PDMS_{11}MA$ | dioxane + 6 vol % DMF | 480 | AGET ATRP | 7 ± 2 [c,e] | 9.61 | 58.6 ± 10 | 132 ± 23 | 0.92 |
| $PDMS_7MA$ [c] | dioxane | 100 | RAFT | 11.5 [c,d,f] | 9.61 | 44 ± 2 | 97 ± 5 | |
| $PDMS_{70}MA$ [c] | dioxane | 100 | RAFT | 11.5 [c,d,f] | 9.61 | 46 ± 1 | 103 ± 4 | |
| $PDMS_{11}MA$ | toluene | 100 | RP | 25 | 2.56 | | | |
| $PDMS_{11}MA$ | toluene | 480 | RP | 12 | 2.56 | | | |
| $PDMS_{11}MA$ | chlorobenzene | 480 | RP | 8.0 | 9.00 | | | |
| $PDMS_{11}MA$ | dioxane | 480 | RP | 6 | 9.61 | | | |
| $PDMS_{11}MA$ | dioxane | 200 | RP | 8 | 9.61 | | | |
| $PDMS_{11}MA$ | dioxane | 100 | RP | 14 | 9.61 | | | |

[a]The difference in total Hansen parameter between PDMS and solvent, calculated based upon the individual Hansen components in Table S7. [b]$\Delta S_p = \Delta S_p^0 + R \ln \frac{[M]_0}{c}$. [c]$[M]_\infty = [M]_{eq}$. [d]Extrapolated from eq 1 using the experimentally calculated $\Delta H_p$ and $\Delta S_p$ parameters. [e]Taken as the average [M] from the 3.5 to 18 h time points due to the low intensity of the macromonomer peak in GPC traces (Figure S7). [f]RAFT data and parameters from ref 21 were extrapolated to $[M]_{eq}$ at 60 °C.

Polymerizations were conducted at different temperatures to independently quantify the effect of the initial starting conditions on $\Delta H_p$ and $\Delta S_p$. The yields in controlled radical polymerizations (CRP) are compared to those determined by conventional "free" radical polymerization (RP) under similar conditions.

ATRP of $PDMS_{11}MA$ was conducted in xylene with $[M]_0 = 480$ mM and 70 °C using $[PDMS_{11}MA]/[dfEBiB]/[CuCl]/[Me_6TREN] = [500]/[1]/[4]/[4]$[41] (480X-70AT). $^1H$ NMR was utilized to track macromonomer consumption by the disappearance of vinyl peaks at 5.56 and 6.11 ppm relative to methylene peaks at 3.3−4.3 ppm (Figure S2). Monomer consumption could also be followed by comparison peak areas between macromonomer and bottlebrush in the same GPC trace (Figure S3). The results from the two methods were comparable (Figure 1). Polymerization was tracked until [M] appeared to reach a plateau near its $[M]_{eq}$ by kinetic plots (Figure 1).[12,21] An example of the approximation using this method is highlighted in Figure 1 for 480X-70AT, where monomer consumption plateaued at [M] = 69 mM after 8 h.

Polymerizations of $PDMS_{11}MA$ at lower temperatures were slower but able to reach higher conversion (Figure S4). 480X-70AT and 480X-45AT had $[M]_{eq}$ of 69 and 22 mM and reached final conversions of 86% and 95%, respectively. The increase in temperature and leaving polymerization at $[M] = [M]_{eq}$ broadened molecular weight distribution of the $PDMS_{11}MA$ bottlebrush due to the increased contribution of depolymerization at its $[M]_{eq}$ (Figure S4).

Model polymerizations in toluene and dioxane were conducted using AGET ATRP with a $Sn(EH)_2$ reducing agent at a molar ratio of $[PDMS_{11}MA]/[EBiB]/[CuBr_2]/[PMDETA]/[Sn(EH)_2] = [50]/[1]/[1]/[3]/[1]$. The 6 v/v% dimethylformamide, which is a poor solvent for PDMSMA ($(\delta_P - \delta_s)^2 = 67.2$), was added to improve catalyst solubility. Polymerization at 60 °C in dioxane (100D-60AG, $(\delta_P - \delta_s)^2 = 9.61$) reached a $[M]_{eq} = 7 \pm 2$ mM, while polymerization in toluene (100Tol-60AG, $(\delta_P - \delta_s)^2 = 2.56$) reached a higher


https://dx.doi.org/10.1021/acsmacrolett.0c00350
ACS Macro Lett. 2020, 9, 1303−1309

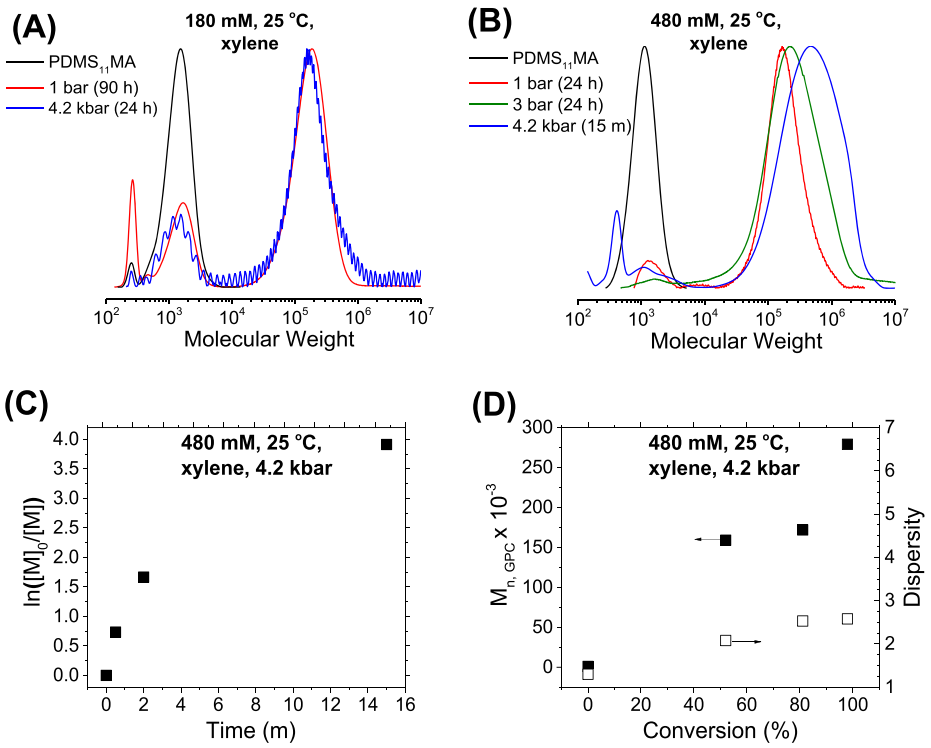


**Figure 3.** Normalized GPC traces of (A) 180X-25AT-4.2K with 180X-25AT and (B) 480X-25AT-4.2kb, 480X-25AT-3K, and 480X-25AT measured by chloroform GPC relative to linear MMA standards. The low molecular weight peak is attributed to the small molecule BHT internal standard used for calibration. (C) First order kinetic plot and (D) number-average molecular weight ($M_{n,GPC}$) vs conversion plot for 480X-25AT-4.2K polymerizations of different time lengths. Conditions: [$PDMS_{11}MA$]/[df-EBiB]/[CuCl]/[$Me_6TREN$] = [500]/[1]/[4]/[4] in xylene at the stated [$PDMS_{11}MA$]$_0$ and $P$.

[M]$_{eq}$ = 28 ± 1 mM (Figure 1). AGET ATRP of $PDMS_{11}MA$ at [M]$_0$ = 480 mM in dioxane (480D-60AG) reached the same [M]$_{eq}$ = 7 ± 3 mM as 100D-60AG, suggesting there is not a significant thermodynamic effect by dilution with a poor solvent between 0.1 and 0.48 M (12−50 vol %). Analogous polymerizations were conducted within a range of 45 to 90 °C to determine the effects of solvent quality on thermodynamic favorability of propagation. Polymerizations at 45 °C (480D-45AG) reached near quantitative conversion due to the very low equilibrium monomer concentration relative to [M]$_0$. The [M]$_{eq}$ of 480D-45AG, 480D-60AG, and 100D-45AG were determined by $^1$H NMR of the last few kinetic points because the residual [$PDMS_{11}MA$] was difficult to distinguish from GPC baseline (Figures S7 and S9). At 90 °C, polymerization reached an [M]$_{eq}$ = 81 mM in toluene and [M]$_{eq}$ ~ 70 mM in dioxane. The [M]$_{eq}$ of 100D-90AG and 100Tol-90AG were also determined by $^1$H NMR because oligomer products overlapped with the macromonomer in the GPC traces (Figure S10).

ln[M]$_{eq}$ was plotted against $1/T$ to determine $\Delta H_p$ and $\Delta S_p^0$ in each solvent according to eq 1 (Figure 2A). $\Delta S_p^0$ was converted to a nonstandard state $\Delta S_p$ by $\Delta S_p = \Delta S_p^0 + R \ln \frac{[M]_0}{c}$. Controlled radical polymerizations of $PDMS_{11}MA$ in poor solvents were more exothermic and exoentropic (Figure 2). Polymerization in xylene was the least favorable, with $\Delta H_p$ and $\Delta S_p$ = −32.6 ± 4 kJ/mol and −67 ± 6 J/mol·K, respectively. Polymerizations in dioxane with 6 vol % of poor solvent DMF ($(\delta_P - \delta_s)^2$ = 67.2) reached the highest yield at low temperature due to a more exothermic and exoentropic reaction. AGET ATRP of $PDMS_{11}MA$ in a mixture of 6 vol % DMF and dioxane was more exothermic and exoentropic than previously reported $\Delta H_p$ and $\Delta S_p$ of $PDMS_{70}MA$ and $PDMS_7MA$ for RAFT polymerizations in pure dioxane (Table 1).[21] This is presumably due to the small addition of DMF to the reaction mixture.

Conventional RPs were conducted using [$PDMS_{11}MA$]:[AIBN] = 50/1 with [$PDMS_{11}MA$]$_0$ = 100−480 mM in toluene, chlorobenzene, and dioxane within a temperature range of 60−90 °C (Table S4). The [M]$_\infty$ values, after approximately 98% of azobis(isobutyronitrile) (AIBN) decomposition, according to reported $k_d$ values, were compared to the [M]$_{eq}$ measured by controlled radical polymerization. At 60 °C, yield was the highest in dioxane, then chlorobenzene and toluene. Polymerization of $PDMS_{11}MA$ in xylene by normal ATRP had an extrapolated [M]$_{eq}$ = 43 mM, which was much larger than [M]$_\infty$ = 6 mM for 480D-60 (Table 1).

RPs at higher [M]$_0$ and [I]$_0$ reached a higher conversion and lower [M]$_\infty$ than analogous CRP experiments. The [M]$_\infty$ of 480D-60 was 6 mM, which was about half of the extrapolated [M]$_{eq}$ = 11.5 mM for RAFT polymerization of PDMSMA macromonomers in pure dioxane. However, 100D-60 reached a [M]$_\infty$ = 14 mM, much closer to the same extrapolated [M]$_{eq}$ = 11.5 mM at the same [M]$_0$ = 100 mM. The [M]$_\infty$ = 12 mM of 480Tol-60 was lower than [M]$_{eq}$ = 28 mM for 100Tol-60AG. More dilute 100Tol-60 reached a [M]$_\infty$ = 25 mM, closer to the thermodynamic [M]$_{eq}$ = 28 mM for 100Tol-60AG.

The differences in [M]$_\infty$ between AGET ATRP and conventional RP prompted us to simulate the kinetics of these polymerizations by PREDICI to unveil the origin of these discrepancies.[43] The simulations are discussed in detail in the Supporting Information. A conventional RP may not reach


https://dx.doi.org/10.1021/acsmacrolett.0c00350
ACS Macro Lett. 2020, 9, 1303−1309

$[M]_{eq}$ and stop at a higher $[M]_{\infty}$ if there is not enough radical initiator. RP can overshoot $[M]_{eq}$ if the initiator concentration is too high, yielding additional oligomeric species. Thus, we stress here that determination of thermodynamic parameters via conventional RP is not fully reliable and may lead to errors if the polymerization conditions are not appropriately selected.[37] The effect of the grafting-through polymerization recipe, kinetic parameters, and transfer on $[M]_{\infty}$ will be investigated in the future.

In summary, the yield of $PDMS_{11}MA$ increased in polymerizations in solvent media with larger differences in total Hansen parameter with PDMS ($(\delta_{PDMS} - \delta_s)^2$). This was due to a more negative $\Delta H_p$, which led to a greater dependence of $[M]_{eq}$ with temperature, but also a more negative $\Delta S_p$. $PDMS_{11}MA$ polymerizations can reach near reaction completion when conducted at high $[M]_0$, in a poor solvent, and at low temperature by suppressing the deleterious effects of the $[M]_{eq}$.

HP-ATRP of $PDMS_{11}MA$ was conducted at ambient temperature with $[PDMS_{11}MA]_0$ = 180, 224, and 480 mM and $P$ = 4.2 or 3 kbar. Polymerization of most vinyl monomers is exothermic and has a negative reaction volume $-\Delta V$, which favorably shifts the propagation−depropagation equilibrium with hydrostatic pressure.[20,29] The overall rate of ATRP also increases with pressure through enhancement of propagation and activation rate coefficients.[44] Radical polymerization at high pressure suppresses diffusion-limited termination pathways by increasing the viscosity of the reaction, effectively decreasing $k_t$ and also increasing $k_p$.[22,45−47] The high-pressure setup utilized in this study did not allow for in situ monitoring of kinetics; thus, polymerizations ran for a set amount of time and $[M]_{eq}$ could not be obtained.

180X-25AT reached 79% conversion after 90 h with good control. Utilizing the same conditions under 4.2 kbar pressure allowed the polymerization to reach 98% conversion by $^1$H NMR in 24 h (180X-25AT-4.2K, Figure 3A). The increase in yield is attributed to a diminished $[M]_{eq}$ at higher pressure as well as kinetic enhancement of propagation relative to termination.[44]

180X-25AT-4.2k had a relatively low dispersity ($M_w/M_n$ = 1.41) with $M_{n,theo}$ = 490000 (Table S8). Further increasing concentration to 224 mM allowed polymerization to reach near quantitative conversion by $^1$H NMR (224X-25AT-4.2K). However, this increase in $[PDMS_{11}MA]_0$ yielded high molecular weight shouldering, presumably caused by slow exchange or termination reactions. 480X-25AT-4.2K reached near quantitative conversion at the expense of an even larger high molecular weight shoulder in 15 min.

Polymerization at a moderate pressure of 3 kbar (480X-25AT-3K) reached a final conversion of 95% after 24 h. GPC spectra show a clear trend in reaction pressure and polymerization control with $[PDMS_{11}MA]_0$ in Figure 3B. Polymerization at 4.2 kbar displayed poor control (480X-25AT-4.2K, $M_w/M_n$ = 2.58). Lowering pressure to 3 kbar moderately improved control over polymerization (480X-25AT-3K, $M_w/M_n$ = 1.77) which was further enhanced by polymerization at ambient pressure (480X-25AT, $M_w/M_n$ = 1.58). The lack of clear boundary conditions suggests poor control is due to kinetic rather than thermodynamic limitations.

Additional ATRPs were repeated at 4.2 kbar with $[PDMS_{11}MA]_0$ = 480 mM to better understand the kinetic limitations of polymerization at high pressure and $[PDMS_{11}MA]_0$ (480X-25AT-4.2K, Table S8). Polymerizations were very fast, reaching 52% conversion in 30 s and near quantitative conversion in 15 min (Figure 3C). Molecular weight and dispersity increased with conversion. The increase in molecular weight with conversion and the absence of low molecular weight tailing in GPC traces suggest efficient initiation and no appreciable transfer occurred (Figure S16). The addition of 0.8 equiv of $CuCl_2$ relative to initiator slightly improved control ($M_w/M_n$ = 2.21), suggesting a higher rate of deactivation could improve control. A hydrophobic BPMODA ligand was employed to enhance the solubility of catalysts at high pressure; however, polymerization was poorly controlled, with a very high dispersity of 6.09 (Table S8, 480X-25AT-4.2KB).

Lower activity CuCl/PMDETA catalyst was also employed (480X-25AT-4.2KP). CuBr/PMDETA has a $K_{ATRP}$ 3 orders of magnitude smaller than CuBr/$Me_6$TREN and a lower volume of reaction (−22 $cm^3$/mol) than $Me_6$TREN (−33 $cm^3$/mol).[44,48] Thus, polymerization with CuCl/PMDETA is slower and should accelerate less with pressure. CuCl/PMDETA improved control over polymerization, lowering dispersity to 1.50 at 90% conversion, but the GPC trace was still bimodal in shape (Figure S17). These results suggest grafting-through polymerization at 4.2 kbar with $[M]_0$ = 480 mM suffers from poor deactivation caused by high viscosity limiting the efficient solubility and mobility of the copper catalyst to deactivate chain ends.

The thermodynamics and kinetics of polymerization were assessed for a sterically hindered poly(dimethylsiloxane) methacrylate ($PDMS_{11}MA$, $M_n$ = 1000) macromonomer as a function of temperature, solvent, initial monomer concentration, and pressure. The $[M]_{eq}$ of a grafting-through polymerization can be mitigated by polymerization at lower temperature in solvents with larger values of $(\delta_{PDMS} - \delta_s)^2$. ATRP and RP of $PDMS_{11}MA$ were more exothermic and exoentropic in dioxane, followed by toluene, and xylene (i.e., in order of increasing $(\delta_{PDMS} - \delta_s)^2$). Simulations of AGET ATRP with a $k_p$ = 815 $M^{-1}$ $s^{-1}$ and $k_t$ = $10^6 \sim 10^8$ $M^{-1}$ $s^{-1}$ showed that AGET ATRP of bulkier macromonomers should reach the equilibrium monomer concentration regardless of initial monomer concentration. However, RP of the same fictional monomers could reach a dead-end polymerization at $[M]_{\infty} > [M]_{eq}$ if all initiator decomposes before reaching $[M]_{eq}$. Oligomers could be made after $[M] = [M]_{eq}$ if the concentration of residual initiator is high enough to initiate a significant amount of new chains, despite depolymerization being favored when $[M] < [M]_{eq}$. The effects of polymerization recipe, kinetic parameters, and transfer on the yield of conventional and controlled radical polymerizations will be investigated in future work.

Application of high pressure significantly improved the yield of grafting-through polymerizations by suppression of $[M]_{eq}$ and termination. Polymerization at $P$ = 4.2 kbar and $[M]_0$ = 480 mM (480X-25AT-4.2K) suffered from lack of control. Systematically lowering pressure from 4.2 kbar to 1 bar decreased the amount of high molecular weight shouldering in GPC traces. Kinetic analysis of 480X-25AT-4.2K showed an increase in molecular weight and dispersity with conversion. The increase in molecular weight with conversion, and the absence of low molecular weight tailing in GPC traces suggested efficient initiation and no appreciable transfer occurred. The addition of $CuCl_2$ (480X-25AT-4.2KCu) and switching to hydrophobic CuCl/BPMODA (480X-25AT-4.2KB) and less active CuCl/PMDETA (480X-25AT-4.2KP)


https://dx.doi.org/10.1021/acsmacrolett.0c00350
ACS Macro Lett. 2020, 9, 1303−1309

resulted in slower reactions with marginally improved control. This suggests that deactivation is likely worse in a grafting-through HP-ATRP at very high $[M]_0$ and $P$ due to very high viscosity, limiting the ability copper catalyst to deactivate chain ends.

## ■ ASSOCIATED CONTENT

### Supporting Information

The Supporting Information is available free of charge at https://pubs.acs.org/doi/10.1021/acsmacrolett.0c00350.

Experimental details and supporting figures and tables (PDF)

## ■ AUTHOR INFORMATION


### Corresponding Author

**Krzysztof Matyjaszewski** − *Department of Chemistry, Carnegie Mellon University, Pittsburgh, Pennsylvania 15213, United States;* orcid.org/0000-0003-1960-3402; Email: matyjaszewski@andrew.cmu.edu

### Authors

**Michael R. Martinez** − *Department of Chemistry, Carnegie Mellon University, Pittsburgh, Pennsylvania 15213, United States*

**Yidan Cong** − *Department of Chemistry, University of North Carolina at Chapel Hill, Chapel Hill, North Carolina 27599-3290, United States*

**Sergei S. Sheiko** − *Department of Chemistry, University of North Carolina at Chapel Hill, Chapel Hill, North Carolina 27599-3290, United States;* orcid.org/0000-0003-3672-1611

Complete contact information is available at: https://pubs.acs.org/10.1021/acsmacrolett.0c00350


### Author Contributions

The manuscript was written through contributions of all authors. All authors have given approval to the final version of the manuscript.

### Notes

The authors declare no competing financial interest.

## ■ ACKNOWLEDGMENTS

K.M. would like to acknowledge financial support from NSF DMR 1921858. S.S. would like to acknowledge financial support from NSF DMR 1921835 and DMR 2004048. M.M. would like to thank Mateusz Olszewski for the introduction to PREDICI and helpful discussions. Kyle Augustine and Dr. Hendrik Schroeder are acknowledged for useful discussions.

## ■ REFERENCES


(1) Sheiko, S. S.; Sumerlin, B. S.; Matyjaszewski, K. Cylindrical molecular brushes: Synthesis, characterization, and properties. *Prog. Polym. Sci.* **2008**, *33* (7), 759−785.

(2) Xie, G.; Martinez, M. R.; Olszewski, M.; Sheiko, S. S.; Matyjaszewski, K. Molecular Bottlebrushes as Novel Materials. *Biomacromolecules* **2019**, *20* (1), 27−54.

(3) Pelras, T.; Mahon, C. S.; Mullner, M. Synthesis and Applications of Compartmentalised Molecular Polymer Brushes. *Angew. Chem., Int. Ed.* **2018**, *57* (24), 6982−6994.

(4) Abbasi, M.; Faust, L.; Wilhelm, M. Comb and Bottlebrush Polymers with Superior Rheological and Mechanical Properties. *Adv. Mater.* **2019**, *31*, 1806484.

(5) Paturej, J.; Sheiko, S. S.; Panyukov, S.; Rubinstein, M. Molecular structure of bottlebrush polymers in melts. *Sci. Adv.* **2016**, *2*, No. e1601478.

(6) Verduzco, R.; Li, X.; Pesek, S. L.; Stein, G. E. Structure, function, self-assembly, and applications of bottlebrush copolymers. *Chem. Soc. Rev.* **2015**, *44* (8), 2405−20.

(7) Sheiko, S. S.; Dobrynin, A. V. Architectural Code for Rubber Elasticity: From Supersoft to Superfirm Materials. *Macromolecules* **2019**, *52* (20), 7531−7546.

(8) Jacobs, M.; Liang, H.; Dashtimoghadam, E.; Morgan, B. J.; Sheiko, S. S.; Dobrynin, A. V. Nonlinear Elasticity and Swelling of Comb and Bottlebrush Networks. *Macromolecules* **2019**, *52* (14), 5095−5101.

(9) Mukherjee, S.; Xie, R.; Reynolds, V. G.; Uchiyama, T.; Levi, A. E.; Valois, E.; Wang, H.; Chabinyc, M. L.; Bates, C. M. Universal Approach to Photo-Crosslink Bottlebrush Polymers. *Macromolecules* **2020**, *53* (3), 1090−1097.

(10) Gao, H.; Matyjaszewski, K. Synthesis of Molecular Brushes by "Grafting onto" Method: Combination of ATRP and Click Reactions. *J. Am. Chem. Soc.* **2007**, *129* (20), 6633−6639.

(11) Gan, W.; Shi, Y.; Jing, B.; Cao, X.; Zhu, Y.; Gao, H. Produce Molecular Brushes with Ultrahigh Grafting Density Using Accelerated CuAAC Grafting-Onto Strategy. *Macromolecules* **2017**, *50* (1), 215−222.

(12) Cho, H. Y.; Krys, P.; Szcześniak, K.; Schroeder, H.; Park, S.; Jurga, S.; Buback, M.; Matyjaszewski, K. Synthesis of Poly(OEOMA) Using Macromonomers via "Grafting-Through" ATRP. *Macromolecules* **2015**, *48* (18), 6385−6395.

(13) Xia, Y.; Kornfield, J. A.; Grubbs, R. H. Efficient Synthesis of Narrowly Dispersed Brush Polymers via Living Ring-Opening Metathesis Polymerization of Macromonomers. *Macromolecules* **2009**, *42* (11), 3761−3766.

(14) Sveinbjörnsson, B. R.; Weitekamp, R. A.; Miyake, G. M.; Xia, Y.; Atwater, H. A.; Grubbs, R. H. Rapid self-assembly of brush block copolymers to photonic crystals. *Proc. Natl. Acad. Sci. U. S. A.* **2012**, *109* (36), 14332−14336.

(15) Shinoda, H.; Miller, P. J.; Matyjaszewski, K. Improving the Structural Control of Graft Copolymers by Combining ATRP with the Macromonomer Method. *Macromolecules* **2001**, *34*, 3186−3194.

(16) Schulz, G. O.; Milkovich, R. Graft Polymers with Macromonomers. I. Synthesis from Methacrylate -Terminated Polystyrene. *J. Appl. Polym. Sci.* **1982**, *27*, 4773−4786.

(17) Beers, K. L.; Gaynor, S. G.; Matyjaszewski, K.; Sheiko, S. S.; Möller, M. The Synthesis of Densely Grafted Copolymers by Atom Transfer Radical Polymerization. *Macromolecules* **1998**, *31* (26), 9413−9415.

(18) Burdyńska, J.; Daniel, W.; Li, Y.; Robertson, B.; Sheiko, S. S.; Matyjaszewski, K. Molecular Bottlebrushes with Bimodal Length Distribution of Side Chains. *Macromolecules* **2015**, *48* (14), 4813−4822.

(19) Xie, G.; Martinez, M. R.; Daniel, W. F. M.; Keith, A. N.; Ribelli, T. G.; Fantin, M.; Sheiko, S. S.; Matyjaszewski, K. Benefits of Catalyzed Radical Termination: High-Yield Synthesis of Polyacrylate Molecular Bottlebrushes without Gelation. *Macromolecules* **2018**, *51* (16), 6218−6225.

(20) Odian, G. *Principles of Polymerization*, 4th ed.; John Wiley & Sons, Inc., 2004.

(21) Flanders, M. J.; Gramlich, W. M. Reversible-addition fragmentation chain transfer (RAFT) mediated depolymerization of brush polymers. *Polym. Chem.* **2018**, *9* (17), 2328−2335.

(22) Rzayev, J.; Penelle, J. Controlled/Living Free-Radical Polymerization under Very High Pressure. *Macromolecules* **2002**, *35*, 1489−1490.

(23) Ivin, K. J.; Dainton, F. S. Some Thermodynamic and Kinetic Aspects of Addition Polymerization. *Q. Rev., Chem. Soc.* **1958**, *12*, 61−92.

(24) Ivin, K. J.; Dainton, F. S. Reversibility of the Propagation Reaction in Polymerizatoin Processes and its Manifestation in the Phenomenon of a 'Ceiling Temperature. *Nature* **1948**, *162*, 705−707.

(25) Neary, W. J.; Isais, T. A.; Kennemur, J. G. Depolymerization of Bottlebrush Polypentenamers and Their Macromolecular Metamorphosis. *J. Am. Chem. Soc.* **2019**, *141* (36), 14220−14229.
(26) Schneiderman, D. K.; Hillmyer, M. A. Aliphatic Polyester Block Polymer Design. *Macromolecules* **2016**, *49* (7), 2419−2428.
(27) Raus, V.; Čadová, E.; Starovoytova, L.; Janata, M. ATRP of POSS Monomers Revisited: Toward High-Molecular Weight Methacrylate−POSS (Co)Polymers. *Macromolecules* **2014**, *47* (21), 7311−7320.
(28) Tu, S.; Choudhury, C. K.; Luzinov, I.; Kuksenok, O. Recent advances towards applications of molecular bottlebrushes and their conjugates. *Curr. Opin. Solid State Mater. Sci.* **2019**, *23* (1), 50−61.
(29) Ivin, K. J. Thermodynamics of Addition Polymerization. *J. Polym. Sci., Part A: Polym. Chem.* **2000**, *38* (12), 2137−2146.
(30) Sawada, H. Thermodynamics of Polymerization. I. *J. Macromol. Sci., Polym. Rev.* **1969**, *3* (2), 313−338.
(31) Small, P. A. The equilibrium between methyl methacrylate and its polymer. *Trans. Faraday Soc.* **1953**, *49*, 441−447.
(32) Ivin, K. J.; Leonard, J. The Effect of Polymer Concentration on the Equilibrium Monomer Concentration for the Anionic Polymerization of a-Methyl Styrene in Tetrahydrofuran. *Eur. Polym. J.* **1970**, *6*, 331−341.
(33) Szymanski, R. Thermodynamics of homogeneous equilibrium copolymerization from the point of view of the Flory-Huggins theory. *Makromol. Chem., Theory Simul.* **1992**, *1*, 129−148.
(34) Penczek, S.; Matyjaszewski, K. Ions and macroesters in the living cationic polymerization of THF. *Journal of Polymer Science, Polymer Symposia* **1976**, *56*, 255−269.
(35) Penczek, S.; Matyjaszewski, K. Kinetics and Mechanism of the Cationic Polymerization of Tetra hydro fur an in Solution. THF-$CH_2Cl_2$ and THF-$CH_2Cl_2$/$CH_3NO_2$ Systems. *Journal of Polymer Science: Polymer Chemistry* **1979**, *17* (8), 2413−2422.
(36) Penczek, S.; Kaluzynski, K. Thermodynamic and Kinetic Polymerizability. *Polymer Science: A Comprehensive Reference* **2012**, *4*, 5.
(37) Martinez, M. R.; Krys, P.; Sheiko, S. S.; Matyjaszewski, K. Poor Solvents Improve Yield of Grafting-Through Radical Polymerization of $OEO_{19}MA$. *ACS Macro Lett.* **2020**, *9*, 674−679.
(38) Haugan, I. N.; Maher, M. J.; Chang, A. B.; Lin, T.-P.; Grubbs, R. H.; Hillmyer, M. A.; Bates, F. S. Consequences of Grafting Density on the Linear Viscoelastic Behavior of Graft Polymers. *ACS Macro Lett.* **2018**, *7* (5), 525−530.
(39) Liang, H.; Morgan, B. J.; Xie, G.; Martinez, M. R.; Zhulina, E. B.; Matyjaszewski, K.; Sheiko, S. S.; Dobrynin, A. V. Universality of the Entanglement Plateau Modulus of Comb and Bottlebrush Polymer Melts. *Macromolecules* **2018**, *51*, 10028.
(40) Daniel, W. F.; Burdynska, J.; Vatankhah-Varnoosfaderani, M.; Matyjaszewski, K.; Paturej, J.; Rubinstein, M.; Dobrynin, A. V.; Sheiko, S. S. Solvent-free, supersoft and superelastic bottlebrush melts and networks. *Nat. Mater.* **2016**, *15* (2), 183−9.
(41) Vatankhah-Varnosfaderani, M.; Keith, A. N.; Cong, Y.; Liang, H.; Rosenthal, M.; Sztucki, M.; Clair, C.; Magonov, S.; Ivanov, D. A.; Dobrynin, A. V.; Sheiko, S. S. Chameleon-like elastomers with molecularly encoded strain-adaptive stiffening and coloration. *Science* **2018**, *359*, 1509−1513.
(42) Jakubowski, W.; Matyjaszewski, K. Activator Generated by Electron Transfer for Atom Transfer Radical Polymerization. *Macromolecules* **2005**, *38*, 4139−4146.
(43) Wulkow, M. Computer Aided Modeling of Polymer Reaction Engineering-The Status of Predici, I-Simulation. *Macromol. React. Eng.* **2008**, *2* (6), 461−494.
(44) Morick, J.; Buback, M.; Matyjaszewski, K. Activation-Deactivation Equilibrium of Atom Transfer Radical Polymerization of Styrene up to High Pressure. *Macromol. Chem. Phys.* **2011**, *212* (22), 2423−2428.
(45) Wang, Y.; Schroeder, H.; Morick, J.; Buback, M.; Matyjaszewski, K. High-pressure atom transfer radical polymerization of n-butyl acrylate. *Macromol. Rapid Commun.* **2013**, *34* (7), 604−9.
(46) Arita, T.; Buback, M.; Janssen, O.; Vana, P. RAFT-Polymerization of Styrene up to High Pressure: Rate Enhancement and Improved Control. *Macromol. Rapid Commun.* **2004**, *25* (15), 1376−1381.
(47) Beuermann, S.; Buback, M.; Russell, G. T. Variation with pressure of the propagation rate coefficient in free-radical polymerization of methyl methacrylate. *Macromol. Rapid Commun.* **1994**, *15*, 351−355.
(48) Morick, J.; Buback, M.; Matyjaszewski, K. Effect of Pressure on Activation-Deactivation Equilibrium Constants for ATRP of Methyl Methacrylate. *Macromol. Chem. Phys.* **2012**, *213* (21), 2287−2292.


https://dx.doi.org/10.1021/acsmacrolett.0c00350
*ACS Macro Lett.* 2020, 9, 1303−1309